Journal of Materials Chemistry A

Accepted Manuscript

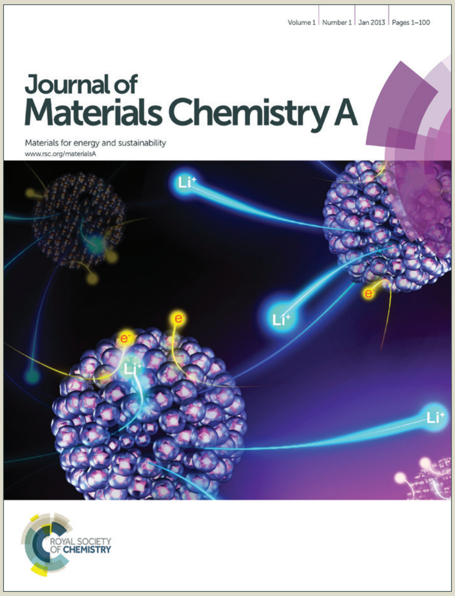

ROYAL SOCIETY OF CHEMISTRY

www.rsc.org/materialsA

Core-Shell Structured Ce_2S_3@ZnO and Their Potential as Pigment

Wen-Xin Mao [a,b], Wei Zhang [b], Zi-Xiang Chi [b], Rong-Wen Lu * [a], An-Min Cao * [b], and Li-Jun Wan * [b]

E-mail address: lurw@dlut.edu.cn, anmin_cao@iccas.ac.cn, wanlijun@iccas.ac.cn

[a] *State Key Laboratory of Fine Chemicals, Dalian University of Technology, Dalian 116024, P. R. China.*

[b] *Key Laboratory of Molecular Nanostructure and Nanotechnology and Beijing National Laboratory for Molecular Sciences, Institute of Chemistry, Chinese Academy of Sciences (CAS), Beijing 100190, P. R. China.*

Abstract

The application of Ce_2S_3 as a promising candidate for nontoxic pigment has long been plagued by its releasing of H_2S. Here we show that a uniform nanoshell of ZnO can effectively eliminate the released H_2S and also improve the thermal stability of Ce_2S_3. Through a series of investigations, a 40 nm ZnO surface coating layer can provide a full protection on the Ce_2S_3 core and best eliminate its H_2S release. Such a core-shell configuration has great potential for the real applications of Ce_2S_3 as an inodorous and nontoxic inorganic pigment.

Key word

Core-shell, thickness control, ZnO coating, Ce_2S_3 pigment, H_2S absorption, thermo-stability

Introduction

Over the past decades, core-shell nanostructures have attracted considerable research interest due to their unique physicochemical properties.[1~5] Generally, the introduction of a surface coating layer can selectively modified the properties of the core materials, leading to a concerted effort from both the core and the shell for optimized performance. Not surprisingly, the core-shell nanostructures can easily find broad applications in different areas including biology, catalysis, energy storage and conversion device.[6~11] For example, a recent progress showed that a surface coating layer of carbon can be pretty effective to alleviate the photo corrosion of CdS.[12] Accordingly, a stable photocatalyst can be successfully prepared. Meanwhile, a surface layer of solid oxide is well known for its capability to improve the thermo-stability of its central core materials.[13, 14]

Inorganic pigments have been widely used in a multitude of industries such as paints, plastics and ceramics. However, those commercially or artistically important pigments usually contain highly toxic heavy metals, typically, CdSe of cadmium red and $PdCrO_4$ of chrome orange. Therefore, it is in emergent need that new types of inorganic pigments without the use of hazardous heavy metals can be developed especially when more strict regulations are being enforced on traditional pigments.[15~17] Recently, people start to discuss the possibility of using rare earth based inorganics as alternative pigments. Typically, Ce_2S_3 is identified as a very promising candidate to replace cadmium and organic red pigments due to its non-toxicity and bright colour.[18] Unfortunately, an inevitable issue that suffers rare earth sulfides is that the corresponding pigments tend to be oxidized to release H_2S. Either a long time exposure to moisture or a high temperature treatment during the injection moulding of pigments will produce unpleasant smell of H_2S, which becomes an enormous challenge for the realistic application of rare earth sulfides. To facilitate the application of Ce_2S_3, some recent efforts begin to introduce a SiO_2 coating on Ce_2S_3 and an enhanced thermal stability has been identified.[19, 20] However, the plaguing effect of H_2S release has hardly been addressed due to the inertness of SiO_2 for H_2S adsorption. To alleviate this problem, different absorbents have been favorable to be used as additives in the pigments.[21, 22] ZnO turns out to be a good choice due to its high sensitivity to H_2S.[23~25] Equally importantly, both ZnO and its reaction product ZnS have a light color so that it will not faint the original one from the pigments.[26]

As far as the protection of Ce_2S_3 is concerned, a core-shell configuration with an inner core of Ce_2S_3 surrounded by a uniform ZnO nanoshell should satisfy the purpose the most. As compared to a simple mixture of Ce_2S_3 and ZnO, which is usually the case for commercially available Ce_2S_3 pigments, the H_2S released from the inner Ce_2S_3 can be absorbed instantaneously by the surrounding ZnO nanoshell without the risk of diffusing out, leading to a possible total elimination of H_2S. Meanwhile, the amount of ZnO necessitated for a total removal of H_2S can be effectively reduced due to a more effective use. In this way, the influence of ZnO on the colour of Ce_2S_3 can be minimized. Interestingly, despite of the obvious advantages of core-shell structures, our literature survey finds no reports on the construction and evaluation of ZnO nanoshells for an improved performance of Ce_2S_3 pigments.

In the present work, a facile synthesis route is adopted for the construction of core-shell nanostructure as Ce_2S_3@ZnO. A uniform and conformal ZnO surface layer is successfully deposited around the core materials of Ce_2S_3, forming an effective absorption layer for H_2S without an obvious degradation on the pigment colour. Our preliminary results show that such a core-shell structure can not only achieve a total absorption of H_2S, but also improve the thermal stability of the Ce_2S_3 core. In this way more thermally-stable pigments can be achieved with a minimized H_2S release, which promises good potential for their realistic applications. Scheme 1 shows the developed process by coating a uniform ZnO nanolayer on Ce_2S_3 core particles.

Results and discussion

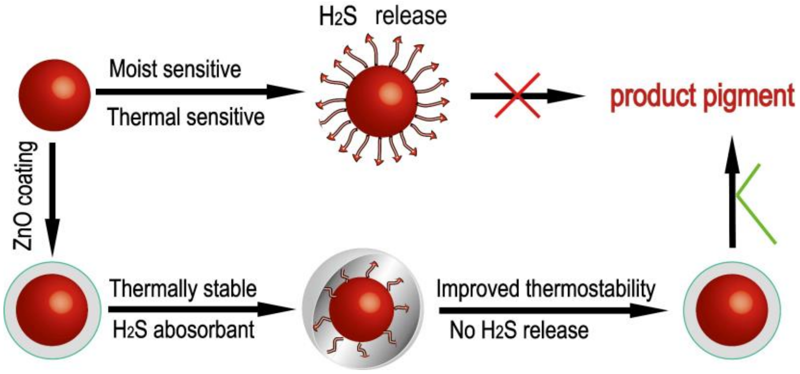

Scheme 1 to show the advantage of a core-shell configuration of Ce_2S_3@ZnO. The ZnO nanoshell can effectively eliminate the released H_2S from Ce_2S_3 and also improve its thermal stability, leading to a more favorable pigment.

The formation of Ce_2S_3@ZnO composites is schematically illustrated in Scheme 1. We used a synthesis route developed by Yang et al., in which ascorbic acid has been selected as an effective ligand and stabilizer to control the gradual formation of ZnO on different metals.[32] We found that this methodology could be well transferred for the coating of Ce_2S_3. The pH value we have used was set at 6.0 so that it would not etch the Ce_2S_3 substrate. Figure 1a shows a scanning electron microscopy (SEM) image of the pristine Ce_2S_3 sample we used (Noted as p-Ce_2S_3). Big chunks of particles with irregular shapes exist as the major morphology for p-Ce_2S_3. A close look by the high magnification SEM reveals that they are not smooth on the surface and there exist smaller particles stacking together (inset in Figure 1a). After the coating treatment, we did not observe an obvious change on the particle shape. However, the SEM image in Figure 1b did reveal that the particles turn much smoother on the surface, which can further be confirmed by HMSEM in inset of Figure 1b. The emergence of a surface layer after the coating process can be clearly revealed by the technique of transmission electron microscopy (TEM). The bare Ce_2S_3 is highly crystalline on the surface with characteristic lattice fringes (Figure S1b). After coating, a distinct nanoshell forms as shown in Figure 1c, circling around the inner particle. The shell thickness is measured to be uniformly 40 nm and the higher resolution TEM (HRTEM) investigation shows that the shell is actually composed of randomly-distributed nanocrystallines with their diameter around 3 nm in Figure S1d. The lattice spacing of a randomly-picked was measured to be 0.26 nm, which consisted with the (002) planes of ZnO structure.[33] The X-ray diffraction characterization on the Ce_2S_3 samples before and after coating did not show obvious peaks from ZnO itself in Figure 1d, probably due to the small crystal size and the very few amount of ZnO (5.43wt %) in the sample.[34,35]

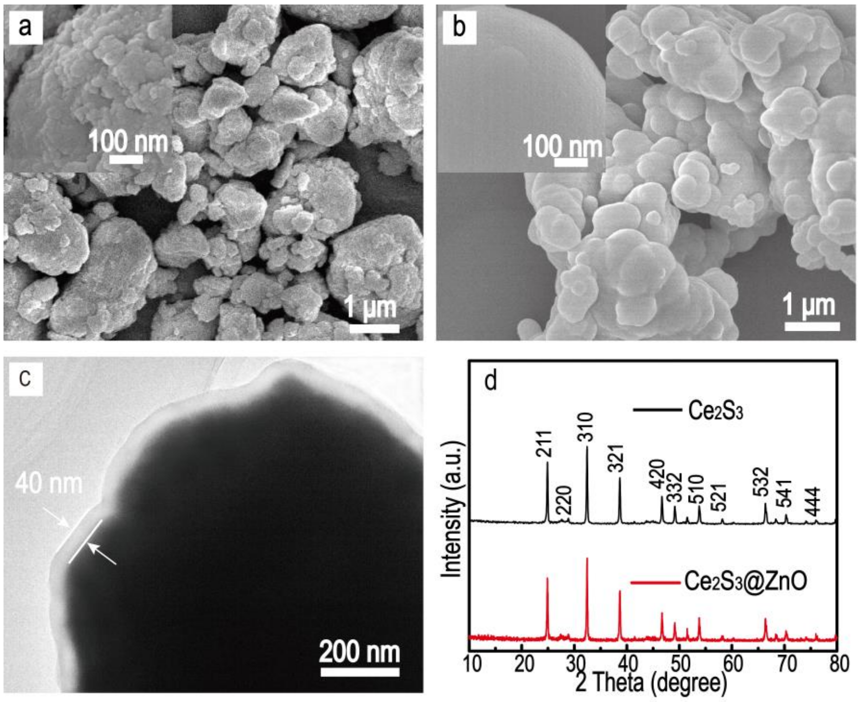

Figure 1 (a) SEM image of Ce_2S_3 pigment. (b) SEM image of Ce_2S_3@ZnO with 40 nm uniform ZnO layer. (c) TEM image of Ce_2S_3@ZnO with 40 nm uniform ZnO layer. (d) XRD pattern of Ce_2S_3 and Ce_2S_3@ZnO.

To further reveal the existence of ZnO on the surface, we did detailed elemental analysis on the core-shell structured sample. Figure 2a shows the energy dispersive spectroscopy (EDS) pattern collected on a representative particle, whose morphology is shown in Figure 2b. This microanalysis technology clearly reveals the existence of ZnO in the Ce_2S_3 sample. Elemental mapping on this sample from Figure 2c-2f further show the locations of different elements. The well-defined spatial distribution confirms a full wrapping of Ce_2S_3 by ZnO, forming a typical core-shell structure of Ce_2S_3@ZnO. It is also noteworthy that all the ZnO species exist as the surface shell without separating into independent nanoparticles. A thorough SEM investigation combined with the elemental analysis on different particles did not find separate particles of ZnO, indicating that all the ZnO exist as the surface shell without phase separating into independent particles.

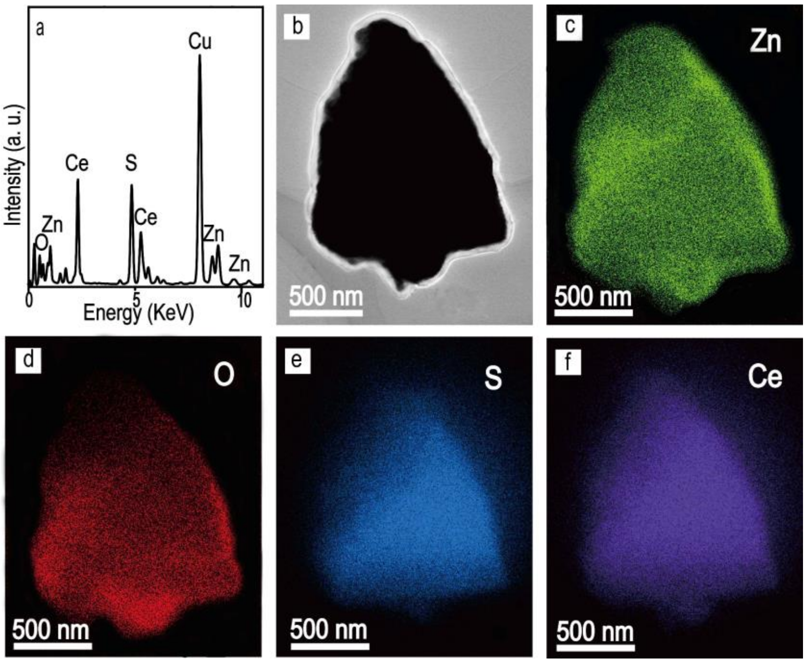

Figure 2 (a) EDS pattern and (b) TEM image of Ce_2S_3@ZnO. The elemental mapping images of Ce_2S_3@ZnO NP in (c) Zn element, (d) O element, (e) S element, (f) Ce element.

The synthesis protocol endows us the capability to easily tune the shell thickness by simply adjusting the concentrations of the reactants. Figure 3a shows a typical TEM image of a thinner ZnO nanoshell when less zinc acetate (4 mM as compared to 10 mM for 40 nm coating) was used. The shell thickness is determined to be 12 nm while the coating still exists as a continuous layer on the surface. The corresponding SEM image (Figure S2) shows a relatively smoother surface compared to that of the p-Ce_2S_3. The underneath granular surface is still discernible due to a thinner coating. Also, nanoshells thicker than 40 nm can be prepared by either increasing the amount of zinc acetate or using a seeded-growth route. Figure 3b shows an 80 nm ZnO shell prepared by using 20 mM zinc acetate. However, due to the colour difference between ZnO and Ce_2S_3, forming a too thick nanoshell is found to be detrimental to the colour of the pigment as will be discussed later in Figure 7d.

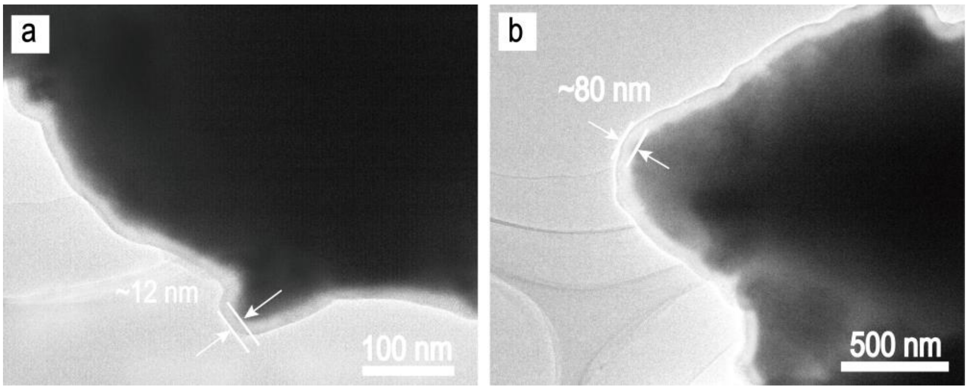

Figure 3 TEM images of (a) Ce_2S_3@ZnO with 12 nm ZnO shell. (b) Ce_2S_3@ZnO with 80 nm ZnO shell.

The existence of a uniform shell can provide an ideal shield for the protection of Ce_2S_3. Typically, such a coating layer can contribute to improving the thermal stability of the p-Ce_2S_3. As shown in Figure 5a, different samples are treated at 380 ^oC to reveal their susceptibility to higher temperatures. For the p-Ce_2S_3, it showed bright red at room temperature (RT) but it quickly turned to grey after heating. The XRD pattern identified the formation of CeO_2 which was due to the oxidation of Ce_2S_3 (Figure 5b). To demonstrate the advantage of core-shell structure, a commercial sample was also tested which consists of a mixture of Ce_2S_3 and ZnO (noted as Ce_2S_3-ZnO in Figure S3). We did not observe an obvious thermal improvement with the existence of ZnO as a separate phase. The colour also turned grey after the heat treatment and CeO_2 showed up as the major product. On the contrary, for the core-shell structured Ce_2S_3@ZnO with 40 nm layer, it is encouraging that the red colour remained nearly intact. Its XRD pattern did not show obvious change after heating, suggesting a much better thermal stability in the presence of the ZnO nanoshells. The better thermal stability of our Ce_2S_3@ZnO sample (40 nm coating) can also be proved by the TGA analysis. As shown in Figure 4, the p-Ce_2S_3 and commercial Ce_2S_3-ZnO had an obvious weight increase attributing to the oxidation of Ce_2S_3 during the heating process. [20] On the contrary, the sample of Ce_2S_3@ZnO did not show this trend as the temperature increase, which manifested the obvious contribution of the ZnO nanoshell. It was noteworthy that we observed a weight loss starting from 350 ^oC for this core-shell structure, which was probably due to the loss of ascorbic acid ligand attached to the ZnO nanoparticles.[32]

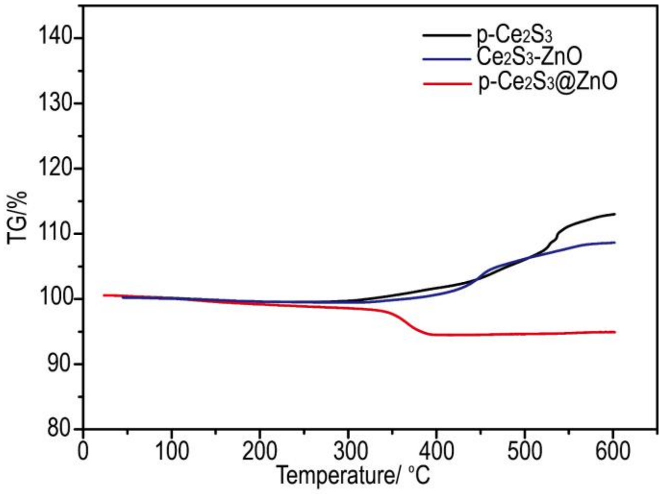

Figure 4 TG analysis of different samples: black line for p-Ce_2S_3; blue line for Ce_2S_3-ZnO and red line for p-Ce_2S_3@ZnO with 40 nm ZnO layer

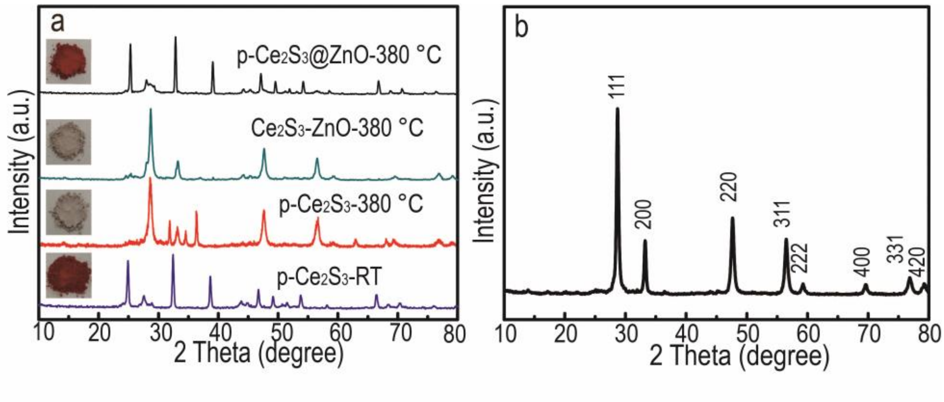

Figure 5 XRD patterns of (a) different materials after calcination at 380 ℃ for 2 h. (b) CeO_2.

For the above-mentioned samples with different configurations, we did systematic tests to evaluate the contribution of ZnO on H_2S removal. For the p-Ce_2S_3, it is not surprising that the amount of released H_2S continued to grow with the temperature increasing (Figure 6). Actually, it was very easy to smell the notorious gas of H_2S when the sample of Ce_2S_3 was being unpacked after a period of storage (e.g., 2 h in a sealed condition). The introduction of a thin coating layer (12 nm TEM image as shown in Figure 3a) can already show its effectiveness towards H_2S removal. Not surprisingly, a thicker ZnO nanoshell will show a better capability in H_2S absorption. For the sample with a 40 nm ZnO shell, it shows very encouraging results and a total removal of H_2S can be achieved. In comparison, we measured the amount of the released H_2S from the commercial sample of Ce_2S_3-ZnO, which was also capable of eliminating the H_2S gas due to the existence of a large amount of ZnO (8.89 wt %) in the sample. However, as temperature increased to 150 ^oC, H_2S signal also emerged due to the accelerated H_2S release at elevated temperature. On the contrary, for the core-shell structured sample of Ce_2S_3@ZnO, there was still no escape of H_2S and its level remained under the detection limit of our instrument. We also note that the ZnO content in Ce_2S_3@ZnO is 5.43 wt %, only 61.52% of the commercial Ce_2S_3-ZnO. It turns out that an uniform ZnO nanoshell can not only contribute to the thermal stability, but also effectively enhance the H_2S control of Ce_2S_3 pigment with much less amount of ZnO.

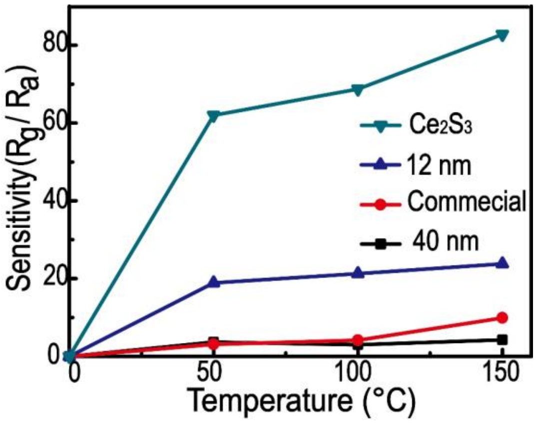

Figure 6 H_2S absorption curves of different materials.

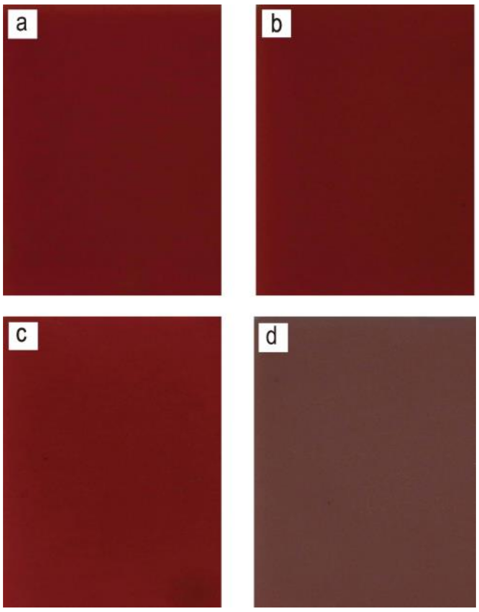

Figure 7 Plastics made from the injection moulding process by using different pigment powders: a) p-Ce_2S_3, b) Ce_2S_3@12nm ZnO, c) Ce_2S_3@40 nm ZnO, d) Ce_2S_3@80nm.

Inspired by the promising performance of Ce_2S_3@ZnO, we carried out preliminary experiment of injection moulding to show its possibility for plastics (Figure 7). The operation is carried out at a high temperature of 200 ^{o}C. For the p-Ce_2S_3, the injection moulding turns out to be a very uncomfortable operation caused by the continuous release of H_2S at 200 ^{o}C, which actually prevents the practical use of p-Ce_2S_3 in real conditions. The 40 nm ZnO can well resolve this problem with no smell of H_2S. The molded plate shows no obvious difference to that of p-Ce_2S_3. It is noticeable that further increase of ZnO layer thickness to 80 nm will induce an apparent change in the plate colour (Figure 7d). Although the colour of the powder itself did not show a huge deviation, this difference will be magnified since only a small amount of pigment powder will be used in the practical industrial operation. A good control on the content of ZnO proves to be significant and the sample with 40 nm shell becomes a best choice as far as a good pigment is expected. The chromaticity data is shown in Table 1. It can be clearly seen that Ce_2S_3@ZnO with 12 nm and 40 nm ZnO layer shows rather little difference with the original Ce_2S_3 pigment on chromaticity (L^*, a^*, b^* difference approximately 1 respectively).[36, 37] However, when the ZnO layer thickness was increased to 80 nm, the chromaticity performance exhibits an obvious decrease compared to the original Ce_2S_3 pigment (ΔL^*: 3.17, Δa^*: 4.21, Δb^*: 3.03).

Table 1 The chromaticity of the original Ce_2S_3 and Ce_2S_3@ZnO with different thicknesses of ZnO layer.

	Ce_2S_3	Ce_2S_3@ZnO 12 nm shell	Ce_2S_3@ZnO 40 nm shell	Ce_2S_3@ZnO 80 nm shell
L^*	43.46	43.18	42.57	40.29
a^*	43.77	43.10	42.85	39.56
b^*	31.36	30.86	30.44	28.33

Conclusion

In summary, a core-shell structured Ce_2S_3@ZnO has been developed to facilitate its application as an inorganic pigment. By means of a facile solution based synthesis route, a uniform and conformal ZnO nanoshell is deposited onto the Ce_2S_3 substrate with the coating thickness being readily tuned. Detailed investigation identified that a 40 nm ZnO surface coating can provide a full protection on the Ce_2S_3 core and eliminate its H_2S release, leading to inodorous powder with much improved thermal stability, which promises a much better potential for its realistic application as a nontoxic inorganic pigment.

Acknowledgements

This work was supported by the major State Basic Research Program of China (973 program: 2013CB934000, 863 program: 2013AA030800), the National Natural Science Foundation of

China (Grant no. 21373238), National Natural Science Foundation of China (Grants No. 21176038), the Chinese Academy of Sciences (XDA09010001). The authors thank the Key Laboratory for Micro-/Nano- Optoelectronic Devices of Ministry of Education, School of Physics and Electronics, Hunan University for the systematic tests to evaluate the contribution of ZnO on H_2S removal and the Beijing Renhe Master Batch Technology Development Center for the injection moulding.

References

1. R. Ghosh Chaudhuri and S. Paria, *Chem. Rev.*, 2011, **112**, 2373-2433.
2. F. Caruso, *Adv. Mater.*, 2001, **13**, 11-15.
3. A. H. Lu, E. L. Salabas and F. Schuth, *Angew. Chem.-Int. Edit.*, 2007, **46**, 1222-1244.
4. Z. C. Sun, E. Zussman, A. L. Yarin, J. H. Wendorff and A. Greiner, *Adv. Mater.*, 2003, **15**, 1929-1933.
5. P. Reiss, M. Protiere and L. Li, *Small*, 2009, **5**, 154-168.
6. M.-C. Daniel and D. Astruc, *Chem. Rev.*, 2003, **104**, 293-346.
7. Q. Zhang, I. Lee, J. B. Joo, F. Zaera and Y. Yin, *Acc. Chem. Res.*, 2012, **46**, 1816-1824.
8. X. Xia, J. Tu, Y. Zhang, X. Wang, C. Gu, X.-b. Zhao and H. J. Fan, *ACS Nano*, 2012, **6**, 5531-5538.
9. F. Tao, M. E. Grass, Y. W. Zhang, D. R. Butcher, J. R. Renzas, Z. Liu, J. Y. Chung, B. S. Mun, M. Salmeron and G. A. Somorjai, *Science*, 2008, **322**, 932-934.
10. Y. Lu, Y. Mei, M. Drechsler and M. Ballauff, *Angew. Chem.-Int. Edit.*, 2006, **45**, 813-816.
11. L. F. Cui, R. Ruffo, C. K. Chan, H. L. Peng and Y. Cui, *Nano Lett.*, 2009, **9**, 491-495.
12. Y. Hu, X. Gao, L. Yu, Y. Wang, J. Ning, S. Xu and X. W. Lou, *Angew. Chem. Int. Ed.*, 2013, **52**, 5636-5639.
13. S. H. Joo, J. Y. Park, C.-K. Tsung, Y. Yamada, P. Yang and G. A. Somorjai, *Nat Mater*, 2009, **8**, 126-131.
14. C.-H. Tsai, S.-Y. Chen, J.-M. Song, I.-G. Chen and H.-Y. Lee, *Corros. Sci.*, 2013, **74**, 123-129.
15. S. Hirai, K. Shimakage, Y. Saitou, T. Nishimura, Y. Uemura, H. Mitomo and L. Brewer, *J. Am. Ceram. Soc.*, 1998, **81**, 145-151.
16. M. A. Perrin and E. Wimmer, *Phys. Rev. B*, 1996, **54**, 2428-2435.

17. I. G. Vasilyeva, B. M. Ayupov, A. A. Vlasov, V. V. Malakhov, P. Macaudiere and P. Maestro, *J. Alloy. Compd.*, 1998, **268**, 72-77.

18. J. M. Tomczak, L. V. Pourovskii, L. Vaugier, A. Georges and S. Biermann, *Proc. Natl. Acad. Sci. U. S. A.*, 2013, **110**, 904-907.

19. G. H. Chen, Z. F. Zhu, H. Liu, Y. F. Wu and C. K. Zhu, *J. Rare Earths*, 2013, **31**, 891-896.

20. S. Y. Yu, D. R. Wang, Y. Liu, Z. Li, X. F. Zhang, X. N. Yang, Y. F. Wang, X. J. Wang and H. Q. Su, *Rsc Advances*, 2014, **4**, 23653-23657.

21. N. Yamazoe, *Sens. Actuator B-Chem.*, 1991, **5**, 7-19.

22. Z. Sun, H. Yuan, Z. Liu, B. Han and X. Zhang, *Advanced Materials*, 2005, **17**, 2993-2997.

23. J. Goclon and B. Meyer, *Physical Chemistry Chemical Physics*, 2013, **15**, 8373-8382.

24. K. X. Yao and H. C. Zeng, *The Journal of Physical Chemistry C*, 2007, **111**, 13301-13308.

25. M. S. Wagh, L. A. Patil, T. Seth and D. P. Amalnerkar, *Mater. Chem. Phys.*, 2004, **84**, 228-233.

26. L. Dloczik, R. Engelhardt, K. Ernst, S. Fiechter, I. Sieber and R. Konenkamp, *Appl. Phys. Lett.*, 2001, **78**, 3687-3689.

27. H. A. Tajmir-Riahi, *J. Inorg. Biochem.*, 1991, **42**, 47-55.

28. S. Xu and Z. L. Wang, *Nano Res.*, 2011, **4**, 1013-1098.

29. H. Sun, J. T. He, J. Y. Wang, S. Y. Zhang, C. C. Liu, T. Sritharan, S. Mhaisalkar, M. Y. Han, D. Wang and H. Y. Chen, *J. Am. Chem. Soc.*, 2013, **135**, 9099-9110.

30. L. Mei, J. Deng, X. Yin, M. Zhang, Q. Li, E. Zhang, Z. Xu, L. Chen and T. Wang, *Sens. Actuators, B*, 2012, **166–167**, 7-11.

31. E. Comini, G. Faglia, G. Sberveglieri, Z. W. Pan and Z. L. Wang, *Appl. Phys. Lett.*, 2002, **81**, 1869-1871.

32. Y. Yang, S. H. Han, G. J. Zhou, L. J. Zhang, X. L. Li, C. Zou and S. M. Huang, *Nanoscale*, 2013, **5**, 11808-11819.

33. H. Zeng, W. Cai, P. Liu, X. Xu, H. Zhou, C. Klingshirn and H. Kalt, *ACS Nano*, 2008, **2**, 1661-1670.

34. N. R. Jana, H.-h. Yu, E. M. Ali, Y. Zheng and J. Y. Ying, *Chem. Commun.*, 2007, 1406-1408.

35. L. Qian, Y. Zheng, J. Xue and P. H. Holloway, *Nat Photon*, 2011, **5**, 543-548.

36. M. Jansen and H. P. Letschert, *Nature*, 2000, **404**, 980-982.

37. D. L. MacAdam, *J. Opt. Soc. Am.*, 1943, **33**, 18-26.

Table of Contents:

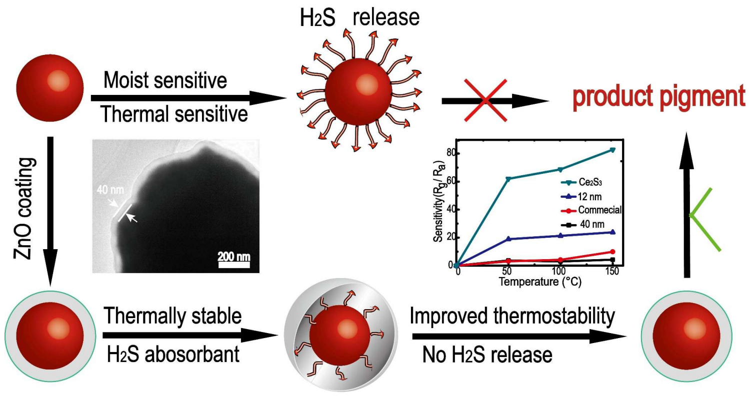

A uniform nanoshell of ZnO can effectively eliminate H_2S and enhance the thermo-stability of Ce_2S_3